

# FATIGUE CRACK GROWTH IN 18G2A STEEL UNDER MIXED MODE I+III LOADING

E. Macha and D. Rozumek  
Technical University of Opole  
ul. Mikołajczyka 5, 45-271 Opole, Poland  
emac@po.opole.pl and drozumek@po.opole.pl

## Abstract

The paper presents the results of tests on fatigue crack growth under proportional bending with torsion in the low-alloy 18G2A steel. Specimens with square sections and stress concentrator in the form of external one-sided sharp notch were used. The tests were performed under the stress ratios  $R = -1, -0.5, 0$ . The test results were described by the  $\Delta J$  integral range and compared with the  $\Delta K$  stress intensity factor range. It has been found that there is a good agreement between the test results and the model of crack growth rate, which includes the  $\Delta J$  integral range.

## Introduction

Analysis of fatigue problems is usually focused on cases of loading causing cracks according to mode I [1, 2]. In practice, we can also observe fatigue crack growth in conditions involving two mixed mode I and II, I and III or II and III, which lead to the material failure. In paper [3], a model for mixed mode (I + III) of fatigue crack growth equivalent to mode I was proposed. Specimens bent in three points were tested, and the crack position was initiated at a certain angle  $\beta$  to the bending plane. Thus, a combination of bending with torsion was obtained. It was found that the crack growth beginning in mode I was dependent on the orientation (direction) and crack opening displacement in the specimen tested. The presented model was proposed by Yates and Miller [4, 5] for circumferential cracks. In [5], there was also shown a behaviour of cracks in the threshold period. Another approach to three-point bending of specimens with a crack for mixed mode I and III was proposed by Pook [6]. Mild steel was tested in the threshold crack range with an expected domination of mode I. In the initial discontinuous changes of mode I were observed, which were followed by a fluent rotation of the crack front up to the moment of an almost perpendicular location to the specimen side. Owing to the increase of the threshold crack in the specimen plane and the cracking stop in the same plane, there appeared some problems with the description of test results as there was no adequate stress intensity factor. The authors of [7] tested the fatigue crack growth in the elastic-plastic material under tension with torsion. The test results were described with the J-integral, using a simple method (force versus deflection) and the finite element method. It was found [7] that the J-integral was the most appropriate fracture mechanics parameter for modes I and III in elastic-plastic materials. A good correlation between the applied methods was obtained.

The aim of this paper is to describe mixed mode I and III crack growth with the  $\Delta J$  integral range and verify the proposed mathematical formula using as an example the test results for 18G2A construction steel.

## Experiments

Flat specimens made of a low-alloy higher-strength steel according to the Polish Standard – PN-86/H-84018 were tested. The specimens were cut of the drawn bar, 16 mm in diameter and their dimensions were: length  $l = 90$  mm, height  $b = 10$  mm, thickness  $g = 8$  mm (see Fig. 1).

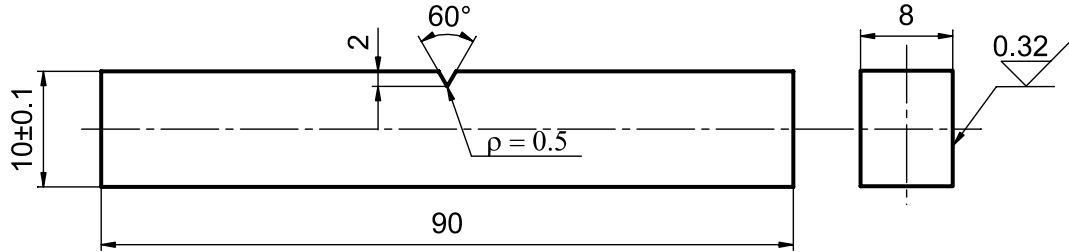


FIGURE 1. Specimen for tests of fatigue crack extension.

The specimens had an external unilateral notch, 2 mm deep and with the rounding radius  $\rho = 0.5$  mm. The tests were performed for the following stress ratios:  $R = -1, -0.5, 0$ . The notches were cut with a cutter and their surfaces were polished after grinding. Chemical composition and some mechanical properties of the tested steel are given in Tables 1 and 2.

TABLE 1. Chemical composition of 18G2A steel.

C - 0.2%	Mn - 1.49%	Si - 0.33%	P - 0.023%	Fe the rest
S - 0.024%	Cr - 0.01%	Ni - 0.01%	Cu - 0.035%	

TABLE 2. Material properties of 18G2A steel.

Yield strength / MPa	Ultimate stress / MPa	Young's modulus / GPa	Poisson's ratio
357	535	210	0.3

Unilaterally restrained specimens were subjected to cyclic bending with torsion with the constant amplitude of moment  $M_a = 17.19$  N·m, which corresponded to the nominal amplitude of normal stress  $\sigma_a = 179$  MPa and the nominal amplitude of shear stress  $\tau_a = 179$  MPa before the crack initiation. The critical value of the integral for 18G2A steel is  $J_{Ic} = 0.331$  MPa·m [8]. Coefficients of the cyclic strain curve under tension-compression in the Ramberg-Osgood equation for 18G2A steel are the following [2]: the cyclic strength coefficient  $K' = 869$  MPa, the cyclic strain hardening exponent  $n' = 0.287$ . The tests were performed on the fatigue test stand MZGS-100 (Fig. 2a) [9] enabling realization of cyclically variable and static (mean) loading. Crack development was observed on the specimen surface with the optical method. The fatigue crack increments were measured with a digital micrometer located in the portable microscope with magnification of 25 times and accuracy 0.01 mm. At the same time, a number of loading cycles  $N$  was written down. Bending with torsion were tested for the ratio of torsional and bending moments  $M_T(t)/M_B(t) = tg\alpha = \sqrt{3}$

(Fig. 2b) and loading frequency 29 Hz. The total moment  $M(t) = 2M_B(t)$  was generated by force on the arm 0.2 m in length.

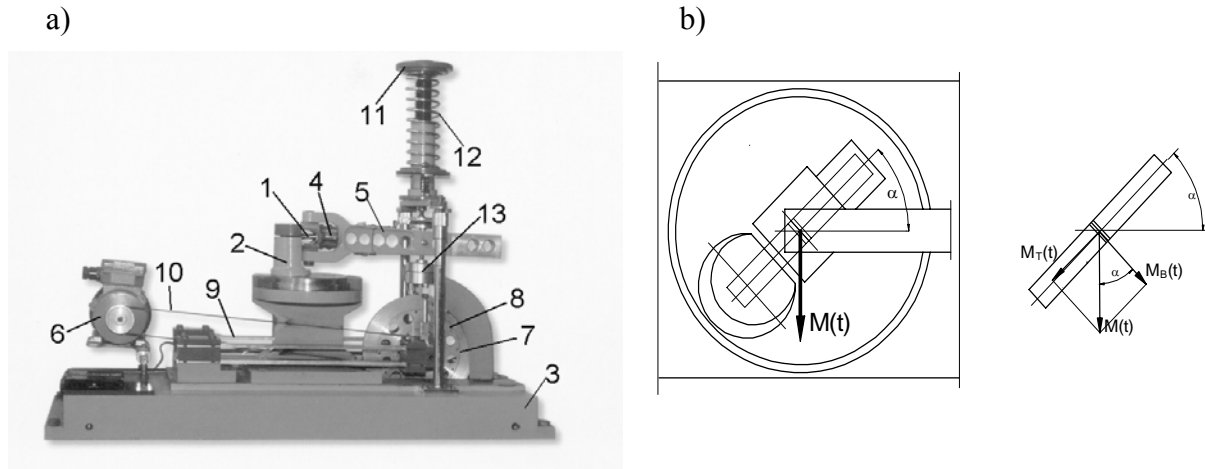


FIGURE 2. Fatigue test stand MZGS-100 a) and loading of the specimen b)

where: 1 – specimen, 2 – rotational head with a holder, 3- bed, 4 - holder, 5 - lever (effective length = 0.2 m), 6 - motor, 7 – rotating disk, 8 - unbalanced mass, 9 – flat springs, 10 – driving belt, 11 – spring actuator, 12 - spring, 13 – hydraulic connector.

The specimen (1) was fixed in holders (2) and (4). Loading was obtained as a result of the lever (5) motion in the vertical plane, generated by inertial force of the unbalanced mass (8) on the rotating disk (7) mounted on flat springs (9). The spring servo-motor (11), mounted on the base (3), enabled giving the mean loading by suitable spring (12) deflection. Mixed modes I and III were obtained by rotation of the head (2) (Fig. 2a) by angle  $\alpha = 60^\circ$  (see Fig. 2b). When  $\alpha = 0^\circ$ , we have pure bending, for  $\alpha = 90^\circ$  we obtain pure torsion.

## The test results and their analysis

The obtained test results allow to analyse fatigue crack growth in 18G2A steel under bending with torsion for different stress ratios  $R = -1, 0.5$  and  $0$ . The tests were performed under controlled loading from the threshold value to the specimen failure. The test results were shown as graphs of the crack length  $a$  versus the number of cycles  $N$  and crack growth rate  $da/dN$  versus the  $\Delta J$  integral range.  $\Delta J$  was compared with the  $\Delta K$  stress intensity factor range. In the case of mixed mode I and III, the range of the equivalent integral  $\Delta J_{eq}$  was assumed, according to [7], as the sum of ranges of integrals  $\Delta J_I$  and  $\Delta J_{III}$

$$\Delta J_{eq} = \Delta J_I + \Delta J_{III} . \quad (1)$$

In the linearly-elastic range, modes I and III were calculated from

$$\Delta J_I = (1 - \nu^2) \Delta K_I^2 / E , \quad (2)$$

$$\Delta J_{III} = (1 + \nu) \Delta K_{III}^2 / E , \quad (3)$$

where  $E$  - Young's modulus,  $\nu$  - Poisson's ratio.

The range of the equivalent stress intensity factor  $\Delta K_{eq}$  under mixed mode I and III reduced to mode I can be written as

$$\Delta K_{eq} = \sqrt{(\Delta K_I^2 \sin \alpha + 2.6 \Delta K_{III}^2 \cos \alpha)}, \quad (4)$$

using the Tresca yield criterion and the Yates relation [3].

The ranges of stress intensity factors  $\Delta K_I$  for mode I and  $\Delta K_{III}$  for mode III are the following:

$$\Delta K_I = \Delta \sigma \sqrt{\pi a} \sin^2 \alpha Y_1(a/w), \quad (5)$$

$$\Delta K_{III} = \Delta \tau \sqrt{\pi a} \sin \alpha \cos \alpha Y_3(a/w). \quad (6)$$

For modes I and III, according to [10] and [11], the correction coefficients take the forms

$$Y_1(a/w) = 5 / \sqrt{20 - 13(a/w) - 7(a/w)^2}, \quad (7)$$

$$Y_3(a/w) = \sqrt{(2w/a) \tan(\pi a / 2w)}, \quad (8)$$

where  $w$  - height of specimen.

$J$ -integrals were calculated with the finite element method (FEM) and the program franc2d in the whole test range as well as the program franc3d in the linearly elastic range in order to compare the influence of thickness for that type of specimens. It was found that there was an influence of the specimen thickness (plane strain), the relative error of the compared methods was below 13%. The cyclic strain curve based on the nonlinear material model was introduced into the program franc2d.

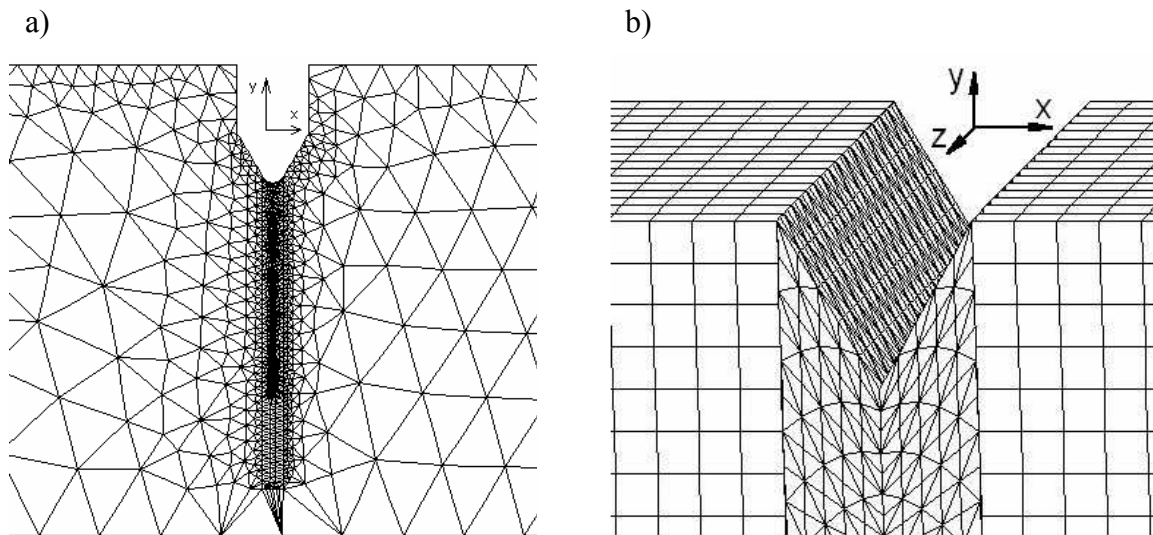


FIGURE 3. Division of the notch region into finite elements in the programs

a) franc2d, b) franc 3d.

The introduced curve was the basis for calculations of stresses, strains and  $J$ -integrals. The calculations were performed for two-dimensional and three-dimensional geometrical models of notched specimens. Fig. 3 shows division of the notch region into finite elements. In the

model presented in Fig. 3a, six-nodal triangular elements were applied, and in the case shown in Fig. 3b ten-nodal quadrilateral elements were used. For calculations, the same loading values as those used in experiments were assumed.

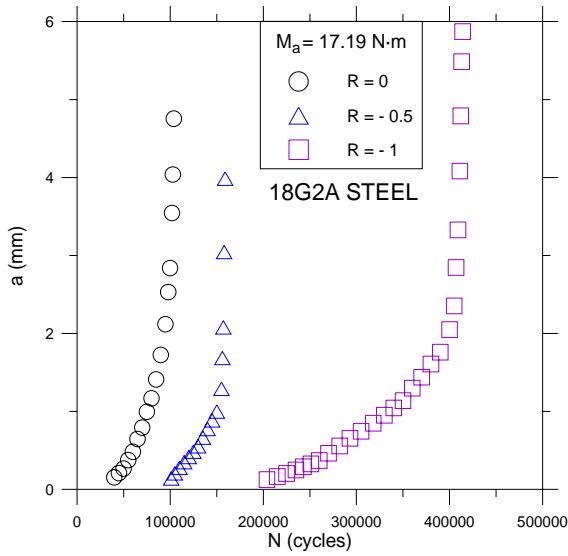


FIGURE 4. Dependences of fatigue crack length  $a$  versus number of cycles  $N$ .

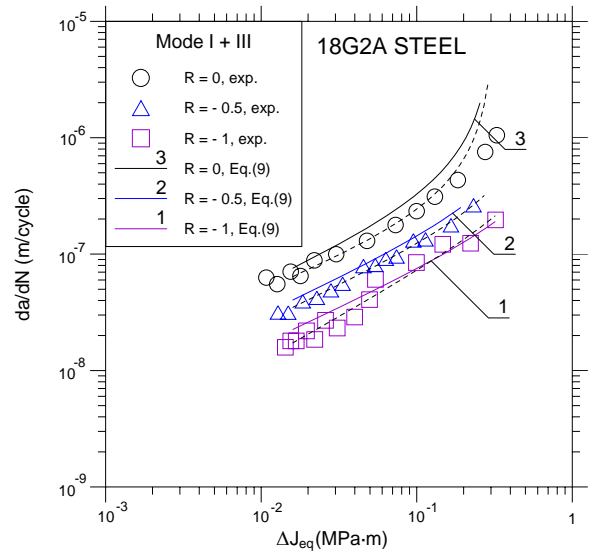


FIGURE 5. Comparison of the experimental results with calculated ones according to Eq. (9).

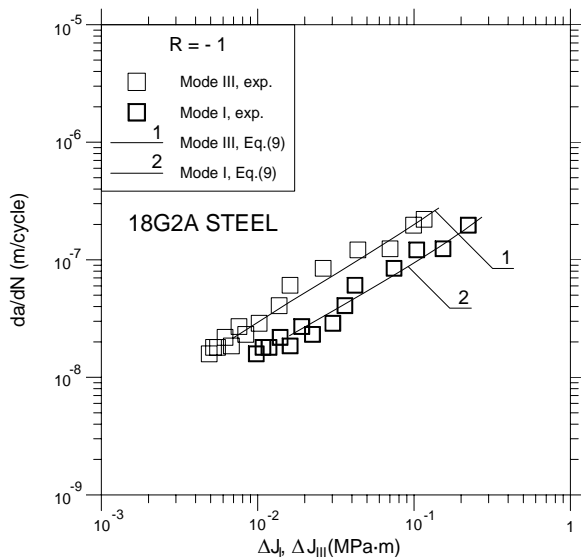


FIGURE 6. Comparison of the experimental results with calculated ones according to Eq. (9).

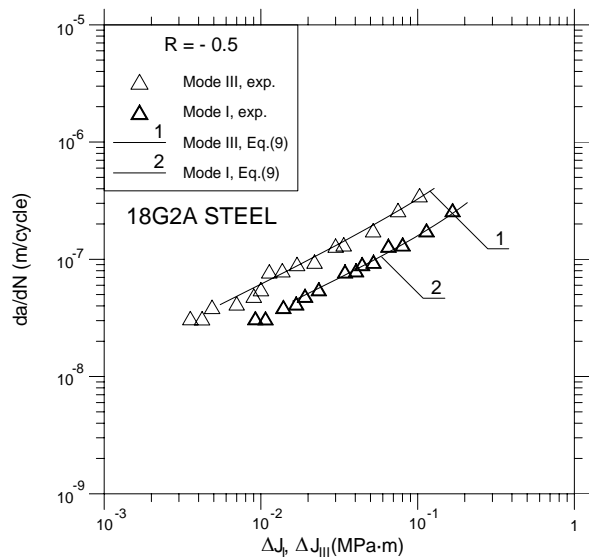


FIGURE 7. Comparison of the experimental results with calculated ones according to Eq. (9).

In the linearly-elastic range, the  $\Delta J_{eq}$  integral ranges calculated from Eqs. (1) – (8) were compared with the results obtained from FEM. The relative error was below 5%. From the

graphs in Fig. 4 it appears that as the stress ratio  $R$  increases from  $-1$  to  $0$ , the fatigue life of the specimens decreases.

The experimental results shown in Figs. 5 to 8 for II and III range of crack growth rate were described with the following model [2]

$$\frac{da}{dN} = \frac{B \left( \frac{\Delta J}{J_0} \right)^n}{(1-R)^2 J_{Ic} - \Delta J} \quad (9)$$

where  $J_{Ic}$  – critical value of the J-integral,  $\Delta J = J_{max} - J_{min}$ ,  $J_0 = 1 \text{ MPa}\cdot\text{m}$  - unit value of the J-integral,  $B$  and  $n$  – coefficients determined experimentally.

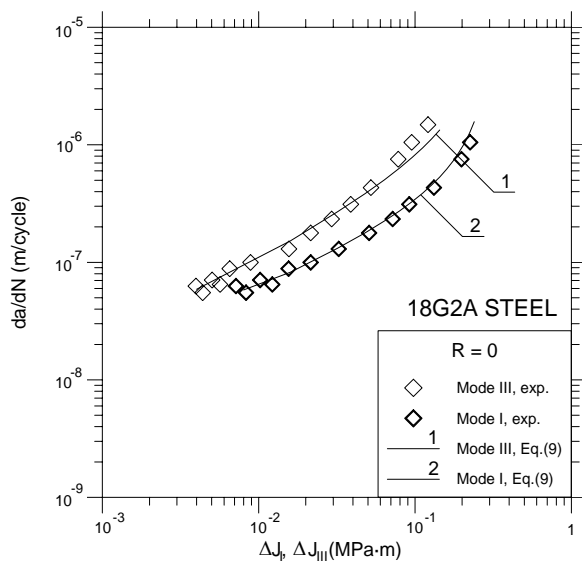


FIGURE 8. Comparison of the experimental results with calculated ones according to Eq. (9).

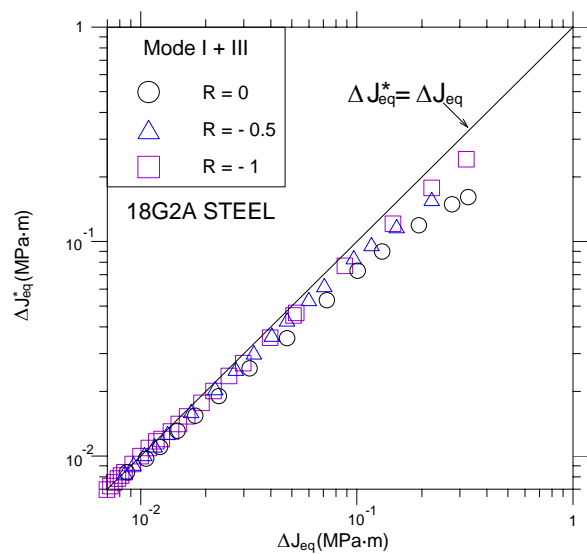


FIGURE 9. The relationship between  $\Delta J_{eq}^*$  and  $\Delta J_{eq}$ .

In Fig. 5 for modes I + III (graphs 1, 2, 3) it can be seen that the change of the stress ratio from  $-1$  to  $0$  is accompanied by the fatigue crack growth rate. The coefficients  $B$  and  $n$  occurring in Eq. (9) were calculated with the least square method and presented in Table 3. It can be seen that for different stress ratios and mixed mode I + III as well as pure modes I and III they take different values. The averaged values of these coefficients are:  $B = 3.5 \cdot 10^{-7} \text{ MPa}\cdot\text{m}^2 / \text{cycle}$  and  $n = 0.62$  (Fig. 5, solid curves). It means that  $B$  and  $n$  are not the material constants but they depend on other factors, like loading or mean value. The test results for cyclic bending with torsion include a relative error not exceeding 20% at the significance level  $\alpha = 0.05$  for the correlation coefficients  $r$  given in Table 3. The coefficients of multiple correlation in all the cases take high values, so there is a significant correlation between the experimental results with the assumed model (9). In Figs. 6 to 8 for different stress ratios, the crack growth rate is expressed versus  $\Delta J$  integral range for pure mode I and for pure mode III. From the graphs in Figs. 6 to 8 it appears that, as in Fig. 5, the change of the stress ratio from  $-1$  to  $0$  causes the crack growth rate. Moreover (Figs. 6, 7 and 8), the fatigue crack growth

rate is higher for mode III than for mode I for the same value of  $\Delta J$ . The model (9) gives satisfactory results for description of the tests.

TABLE 3. Coefficients  $B$ ,  $n$  of model (9) and correlation coefficients  $r$  for the curves shown in Figs. 5 – 8.

Fig.	$B$ [MPa · m <sup>2</sup> / cycle]	$n$	$r$
Fig. 5 – 1(broken curve)	$4.81 \cdot 10^{-7}$	0.75	0.98
Fig. 5 – 2(broken curve)	$3.20 \cdot 10^{-7}$	0.62	0.99
Fig. 5 – 3(broken curve)	$1.90 \cdot 10^{-7}$	0.55	0.99
Fig. 6 – 1(solid curve)	$1.45 \cdot 10^{-6}$	0.79	0.99
Fig. 6 – 2(solid curve)	$6.10 \cdot 10^{-7}$	0.74	0.98
Fig. 7 – 1(solid curve)	$9.45 \cdot 10^{-7}$	0.67	0.99
Fig. 7 – 2(solid curve)	$4.40 \cdot 10^{-7}$	0.64	0.99
Fig. 8 – 1(solid curve)	$9.90 \cdot 10^{-7}$	0.74	0.99
Fig. 8 – 2(solid curve)	$3.00 \cdot 10^{-7}$	0.60	0.99

Calculating  $\Delta J_{eq}$  integral range for mixed mode I + III, we can find that there is a functional relation between the loading range, the elastic-plastic strain range, the crack opening and the crack length. Great values correlation coefficients show that all these factors were approximately included. Above a certain value of  $\Delta J_{eq}$  integral range the crack growth rate without further increase of this integral range. Such behaviour is connected with a unstable crack growth rate in the final stage of the specimen life. In this period, also the stress drop can be observed as plasticization increases. Application of the  $\Delta J$  parameter is reasonable in the case of elastic-plastic materials and those with a distinct yield point. In order to prove applicability of  $\Delta J$ , the authors analysed correlation between the parameters  $\Delta K_{eq}$  and  $\Delta J_{eq}$ . The following relation was used

$$\Delta J_{eq}^* = (1 - \nu^2) \frac{\Delta K_{eq}^2}{E} \quad (10)$$

Fig. 9 shows the relation between the parameters  $\Delta J_{eq}^*$  and  $\Delta J_{eq}$  for three stress ratios  $R$ . A good linear relation (in the double logarithmic system) between these two parameters in the case of the fatigue crack growth rate the tested material for  $\Delta J_{eq} < 1 \cdot 10^{-2}$  MP·m. It means that in this test range under controlled loading, the parameter  $\Delta J_{eq}$  plays a similar role as the parameter  $\Delta K_{eq}$  up to the moment when plastic strain occurs. When plastic strains increase, we can find the increasing difference between  $\Delta J_{eq}^*$  and  $\Delta J_{eq}$ . The difference results from the fact that the parameter  $\Delta J_{eq}^*$  does not include plastic strains. At the final stage of the specimen life, when  $\Delta J_{eq}$  integral range approaches to the critical value of  $J_{Ic}$ , the crack growth rate rapidly (Fig. 9,  $R = 0$ ) and leads to the material failure.

## Conclusions

From the test results for fatigue crack growth in 18G2A steel under proportional cyclic bending with torsion, the following conclusions can be drawn:

1. The applied model (9) including  $\Delta J$  integral range is good for description of fatigue crack growth rate tests in modes I and III and in mixed mode I + III.
2. It has been shown that the applied parameter  $\Delta J_{eq}$  as compared with the parameter  $\Delta K_{eq}$  for different stress ratios R is better for description of crack growth rate in 18G2A steel.
3. It has been found that mode III has a higher crack growth rate than mode I in the tested material. It has been proved that a change of the stress ratio from  $R = -1$  to  $R = 0$  causes the fatigue crack growth rate.

## References

1. Macha, E. and Rozumek, D., *International Conference on Fatigue Crack Paths*, edited by A. Carpinteri, Parma, 2003, 8-16.
2. Rozumek, D., *Materials Engineering*, Zilina, vol. **10**, 1-8, 2003
3. Yates, J.R., *Int. J. Fatigue*, vol. **13**, 383-388, 1991
4. Yates, J.R. and Miller, K.J., *Fatigue Fract. Eng. Mater. Struct.* vol. **11**, 321-330, 1988
5. Yates, J.R. and Miller, K.J., *Fatigue Fract. Eng. Mater. Struct.* vol. **12**, 259-270, 1989
6. Pook, L.P., *Int. J. Fatigue*, vol. **7**, 21-30, 1985
7. Kimachi, H., Tanaka, K., Akiniwa, Y. And Yu, H., *International Conference on Fatigue Crack Paths*, edited by A. Carpinteri, Parma, 2003, 8-16.
8. ASTM E813 – 89, *American Society for Testing and Materials*, Philadelphia, 1987.
9. Achtelik, H. and Jamroz, L., *Patent PRL No.112497, CSR No.200236 and HDR No.136544*, Warsaw, Poland, 1982.
10. Harris, D.O., *J. Bas. Engng.*, vol. **89**, 1967
11. Chell, G.G. and Girvan, E., *Int. J. Fracture*, vol. **14**, R81-R84, 1978

**Acknowledgements:** This work was supported by the Commission of the European Communities under the FP5, GROWTH Programme, contract No. G1MA-CT-2002-04058 (CESTI)